

Selective Oxidation of 1,2-Propanediol to Carboxylic Acids Catalyzed by Copper Nanoparticles

Wuping Xue¹, Hengbo Yin^{1,*}, Zhipeng Lu¹, Aili Wang^{1,*}, Shuxin Liu², and Lingqin Shen¹

¹Faculty of Chemistry and Chemical Engineering, Jiangsu University, Zhenjiang 212013, China

²School of Chemistry and Chemical Engineering, Mianyang Normal University, Mianyang, 621000, China

Copper nanoparticles with different particle sizes were prepared by a wet chemical reduction method in the presence of organic modifiers, such as citric acid (CA), hexadecyl trimethyl ammonium bromide, Tween-80 (Tween), and polyethylene glycol 6000. Selective oxidation of sustainable 1,2-propanediol with O₂ to high-valued lactic, formic, and acetic acids catalyzed by the copper nanoparticles in an alkaline medium was investigated. The small-sized Cu_{CA} nanoparticles with the average particle size of 15.2 nm favored the formation of acetic and formic acids while the Cu_{Tween} nanoparticles with the average particle size of 26.9 nm were beneficial to the formation of lactic acid. The size effect of copper nanoparticles on the catalytic oxidation of 1,2-propanediol to the carboxylic acids was obvious.

Keywords: Copper Nanoparticles, Lactic Acid, Acetic Acid, Formic Acid, 1,2-Propanediol.

IP: 178.165.84.105 On: Sun, 17 Jun 2018 06:19:29

Copyright: American Scientific Publishers

Delivered by Ingenta

1. INTRODUCTION

Fossil fuels, as the main traditional resources, can hardly meet the rapidly increased energy demand and cause many environmental impacts that limit human wellbeing.^{1,2} Biomass is one of renewable resources and can be used to produce various valuable chemicals. Utilizing renewable and low-cost biomass for the production of chemicals has greatly aroused the attention of researchers.¹⁻⁷

Glycerol, a by-product in biodiesel production, can be converted to 1,2-propanediol, acrolein, triacetyl glycerol, and glyceric acid via various processes.⁸⁻¹³ 1,2-Propanediol with a yield of more than 90% is easily synthesized through the hydrogenolysis of glycerol.^{9,10} 1,2-Propanediol is also coproduced in the dimethyl carbonate production by the transesterification method. At present, 1,2-propanediol is facing a severe overcapacity problem because of its scant demand in the production of organic solvent and unsaturated polyester resin.¹⁴ Oxidation of 1,2-propanediol to lactic, formic, and acetic acids was highlighted over the past several years because these three organic acids are basic raw materials in the chemical industry.

Lactic acid has abundant applications in the food, pharmaceutical, and biodegradable plastic industries.¹⁵⁻¹⁷

Lactic acid is conventionally manufactured by the carbohydrate fermentation method at a low reaction rate and a high cost.^{17,18} Formic acid and acetic acid are both important organic chemicals used in the pharmaceutical and agricultural industries in high demand.¹⁹ Formic acid and acetic acid are conventionally produced via the oxidation and carbonylation of methanol, respectively. Methanol is produced using unrenovable natural gas and coal as the starting materials. Developing new sustainable processes for the production of lactic, formic, and acetic acid is worth of investigation.

Recently, the preparation and utility of nanomaterials in the fields of catalysis, pollutant treatment, drug delivery, gas sensor, and energy storage have attracted a great attention of researchers.²⁰⁻²⁸ Especially in the catalysis field, it is found that nanosized catalysts exhibit distinguished catalytic performances as compared with their bulks.²³⁻²⁶ In previous reported work, oxidation of 1,2-propanediol was generally catalyzed by noble metal catalysts, such as Au,^{14, 15, 29-34} Pd,^{14, 15, 21, 33, 35} Pt,^{34, 36} Ag,^{35, 37} etc. These catalysts exhibited good catalytic activities for the oxidation of 1,2-propanediol to lactic acid. However, the noble metal catalysts are pretty expensive, limiting their practical applications. To the best of our knowledge, the catalytic performances of non-noble metal catalysts for the oxidation of 1,2-propanediol have not been reported. Among non-noble metal catalysts, metallic Cu⁰

*Authors to whom correspondence should be addressed.

nanoparticles have many advantages, such as low cost, high stability, and high catalytic activity, under mild reaction conditions.³⁸ Furthermore, the morphologies and particle sizes of metallic Cu⁰ nanoparticles significantly affect their catalytic performances. The catalytic performances of metallic Cu⁰ nanoparticles for the oxidation of 1,2-propanediol are worth of investigation.

In our present work, metallic Cu⁰ nanoparticles were prepared by a wet chemical reduction method in the presence of different-structured organic modifiers and used to catalyze the oxidation of 1,2-propanediol with O₂ in an alkaline aqueous solution. The metallic Cu⁰ nanoparticles were characterized by XRD, XPS, and TEM techniques. The effect of the particle sizes of metallic Cu⁰ nanoparticles and reaction parameters on the catalytic oxidation of 1,2-propanediol was investigated in detail.

2. EXPERIMENTAL DETAILS

2.1. Materials

Sodium hydroxide (NaOH), hydrazine hydrate (N₂H₄ · H₂O), copper nitrate (Cu(NO₃)₂ · 3H₂O), sodium dihydrogen phosphate (NaH₂PO₄), phosphoric acid (H₃PO₄, 85%), hydrochloric acid (HCl), citric acid (C₆H₈O₇, CA), hexadecyl trimethyl ammonium bromide (C₁₉H₄₂BrN, CTAB), polyoxyethylene sorbitan monooleate (Tween-80) (C₂₄H₄₄O₆, Tween), polyethylene glycol (HO(CH₂CH₂O)_nH, average Mn 6000, PEG), 1,2-propanediol, lactic acid, formic acid, acetic acid, and ethanol were of reagent grade and were purchased from Sinopharm Chemical Reagent Co., Ltd. China. Methanol was of chromatographic grade and was purchased from Sinopharm Chemical Reagent Co., Ltd. China. All the chemicals were used as received without further purification.

2.2. Preparation of Copper Nanoparticles

Copper nanoparticles were prepared starting from copper nitrate using CA, CTAB, Tween, and PEG as the organic modifiers and hydrazine hydrate as the reductant, respectively. The preparation procedures are described as follows: 1.89 g of copper nitrate and 0.19 g of organic modifier were dissolved in 70 mL of anhydrous ethanol under ultrasonic treatment. After the mixture was heated at 60 °C for 10 min, 40 mL of NaOH (1.2 M) ethanol solution was added dropwise into it to adjust the pH value of the reaction solution to 8–9. Then, ethanol solution of hydrazine hydrate (8.0 mL hydrazine hydrate in 100 mL anhydrous ethanol) was added dropwise into the mixture and kept at 60 °C for 2 h under mild stirring. The color of the reaction solution changed to black, indicating that Cu²⁺ was reduced to metallic Cu⁰. The resultant metallic copper nanoparticles were cooled to room temperature and kept in anhydrous ethanol. The metallic copper nanoparticles were centrifugated, washed with anhydrous ethanol, and dried at 40 °C in a vacuum oven overnight before

they were characterized and used as the catalysts for the oxidation of 1,2-propanediol.

The as-prepared metallic copper nanoparticles using CA, CTAB, Tween, and PEG as the organic modifiers were denoted as Cu_{CA}, Cu_{CTAB}, Cu_{Tween}, and Cu_{PEG}, respectively. Metallic copper nanoparticles were also prepared without the use of organic modifier, which were denoted as Cu₀.

2.3. Characterization

The crystal phases of the as-prepared copper nanoparticle samples were determined by the powder X-ray powder diffraction (XRD), which were recorded on a diffractometer (D8 super speed Bruke-AEX Company, Germany) using Cu K α radiation ($\lambda = 1.54056 \text{ \AA}$) with a Ni filter at room temperature. The scanning range was from 20° to 80° (2 θ). The crystallite sizes of metallic copper samples, (111) plane, were calculated by using the Scherrer's equation: $D = K\lambda / (B \cos \theta)$, where K was taken as 0.89 and B was the full width of the diffraction line at half of the maximum intensity. The metallic Cu (111) crystallite sizes of the samples are listed in Table I.

Transmission electron microscopy (TEM) images were obtained on a microscope (JEM-2100) operated at an acceleration voltage of 200 kV to characterize the morphologies and crystal structures of the copper nanoparticles. Specimens for TEM analysis were prepared by suspending the copper nanoparticles in ethanol and mounting droplets of the suspension on a copper grid coated with a layer of amorphous carbon. The data used for the calculation of the particle size distribution for each sample was measured from the TEM and HRTEM images. The average particle sizes of metallic Cu⁰ nanoparticles were calculated by a weighted-average method according to the individual particle sizes of the all counted particles.

X-ray photoelectron spectra (XPS) of the metallic Cu⁰ nanoparticles were obtained on a Thermo ESCALAB 250 spectrometer using Al K α radiation (1486.6 eV). The binding energies were calculated with the respect to C1s peak of contaminated carbon at 284.6 eV.

2.4. Catalytic Test

Catalytic oxidation of 1,2-propanediol with O₂ was carried out in a 1000 mL capacity stainless steel autoclave with a magnetically driven impeller and a cooling coil. Appointed amounts of 1,2-propanediol, sodium hydroxide, metallic copper nanoparticle catalyst, and water were added into the autoclave. Firstly, the autoclave was purged with nitrogen for 10 min to replace the air inside. After a given reaction temperature was reached at a stirring speed of 100 rpm (for heating evenly), pure O₂ was introduced to a desired pressure and the catalytic oxidation of 1,2-propanediol started at a stirring speed of 600 rpm. After reacting for a given time period, the autoclave was cooled to room temperature and depressurized for product analysis.

The concentration of remained 1,2-propanediol was analyzed on a gas-phase chromatograph (SP-6800A) equipped

Table I. The catalytic activities of Cu nanoparticles for the oxidation of 1,2-propanediol.

Catalysts	Organic modifiers	Crystallite sizes of Cu (111) (nm)	Average particle sizes (nm)	Binding energies (eV)		Conversions ^a (%)	Selectivities (%)			TOF ^b (h ⁻¹)
				Cu2p _{1/2}	Cu2p _{3/2}		Lactic acid	Acetic acid	Formic acid	
Cu _{CA}	CA	18.9	15.2	952.2	932.2	89.9	38.6	40.5	16.1	4.02
Cu _{CTAB}	CTAB	23.1	24.5	952.4	932.5	85.7	48.3	35.1	12.7	3.84
Cu _{Tween}	Tween	24.0	26.9	952.3	932.4	83.8	52.4	31.8	11.4	3.75
Cu _{PEG}	PEG	27.7	36.5	952.5	932.6	80.3	47.1	35.2	10.6	3.60
Cu ₀	/	34.4	47.1	952.5	932.6	77.1	43.3	38.1	6.3	3.45

Notes: ^aReaction conditions: 1,2-propanediol aqueous solution, 200 mL, 0.14 mol L⁻¹; NaOH concentration, 0.28 mol L⁻¹; O₂ pressure, 1.0 MPa; catalyst loading, 0.1 g; reaction temperature, 200 °C; reaction time, 4 h; and stirring rate, 600 rpm. ^bTOF = The moles of converted 1,2-propanediol divided by moles of Cu catalysts and reaction time.

with a PEG-20 M packed capillary column (0.25 mm × 30 m) and a FID detector by the internal standard method with *n*-butanol as the internal standard. Before product analysis, the reaction mixture was filtrated and the filtrate was acidified with a hydrochloric acid (12 M) to a pH value of *ca.* 3. The products, such as formic acid, lactic acid, and acetic acid, were analyzed on a Varian HPLC system equipped with a reverse-phase column (Chromspher 5 C18, 4.6 mm × 250 mm) and a UV detector set at a wavelength of 210 nm and 30 °C. The eluent was composed of H₃PO₄/NaH₂PO₄ (0.1 M NaH₂PO₄ acidified by H₃PO₄ to a pH value of 2.3) buffer aqueous solution and methanol of chromatographic grade (V:V = 9:1), and the flow rate was 0.8 mL min⁻¹. The concentrations of products were analyzed by the external standard method. The product selectivities were calculated on carbon balance and the equation is listed as follows.

$$S_i = n_i \times n_c / 3(n_0 - n_t)$$

where S_i is the selectivity of product i ; n_i is the mole number of formed product i , mol; n_c is the carbon number of product molecule; n_0 is the initial mole number of 1,2-propanediol, mol; n_t is the mole number of remained 1,2-propanediol at reaction time t , mol.

3. RESULTS AND DISCUSSION

3.1. XRD Analysis

The X-ray powder diffraction patterns of the copper nanoparticles prepared in the presence CA, CTAB, Tween, and PEG as the organic modifiers are shown in Figure 1. Three diffraction peaks in the XRD spectra of the copper nanoparticles were observed. The diffraction peaks appearing at $2\theta = 43.3^\circ$, 50.4° , and 74.1° were indexed as the (111), (200), and (220) planes of the face centered-cubic (fcc) copper, respectively (JCPDS 04-0836). No diffraction peaks of copper oxides or copper hydroxides were detected, indicating that phase-pure metallic Cu⁰ nanoparticles were prepared under our present experimental conditions.

The Cu (111) crystallite sizes of the copper nanoparticles were estimated by Scherrer's equation (Table I).

The crystallite sizes of the Cu nanoparticles ranged from 18.9 to 34.4 nm. The crystallite sizes were in an order of Cu_{CA} (18.9 nm) < Cu_{CTAB} (23.1 nm) < Cu_{Tween} (24.0 nm) < Cu_{PEG} (27.7 nm) < Cu₀ (34.4 nm). The results revealed that the presence of organic modifiers with different functional groups caused the formation of the metallic copper nanoparticles with different crystallite sizes, probably due to the different interactions between organic modifiers and copper or copper hydroxide crystallites.

3.2. TEM Analysis

The TEM images of the copper nanoparticles prepared with the use of CA, CTAB, Tween, and PEG as the organic modifiers and without the use of an organic modifier are shown in Figures 2(a1)–(e1). The average particle sizes of the copper nanoparticles were *ca.* 15.2, 24.5, 26.9, 36.5, and 47.1 nm, respectively. And the particle size distributions were 8.7–25.8, 14.3–35.9, 15.5–42.7, 19.6–50.9, and 24.4–75.8 nm, respectively. The average particle sizes were in an order of

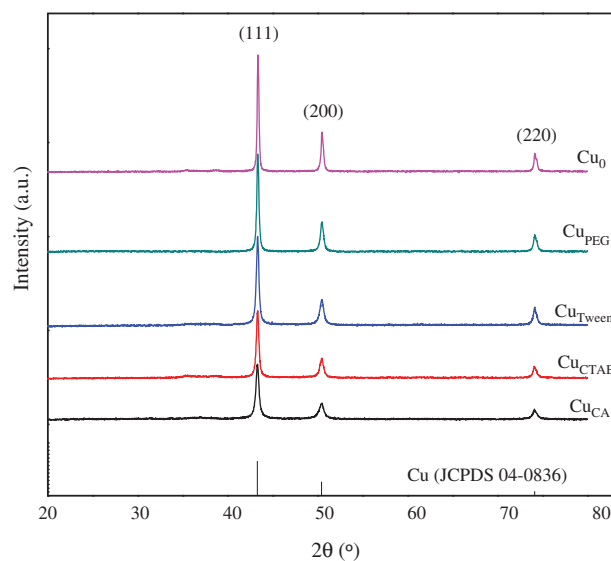


Figure 1. XRD patterns of copper nanoparticles prepared with the use of CA, CTAB, Tween, and PEG as the organic modifiers and without an organic modifier.

$\text{Cu}_{\text{CA}} < \text{Cu}_{\text{CTAB}} < \text{Cu}_{\text{Tween}} < \text{Cu}_{\text{PEG}} < \text{Cu}_0$, which was consistent with that obtained by XRD analysis.

The HRTEM and SAED images (Figs. 2(a2–e2)) show that the diffraction fringes were examined to be *ca.* 0.208,

0.180, and 0.128 nm, close to the {111}, {200}, and {220} lattice spacings of fcc metallic copper, respectively, indicating that the as-prepared copper nanoparticles had polycrystalline structure.

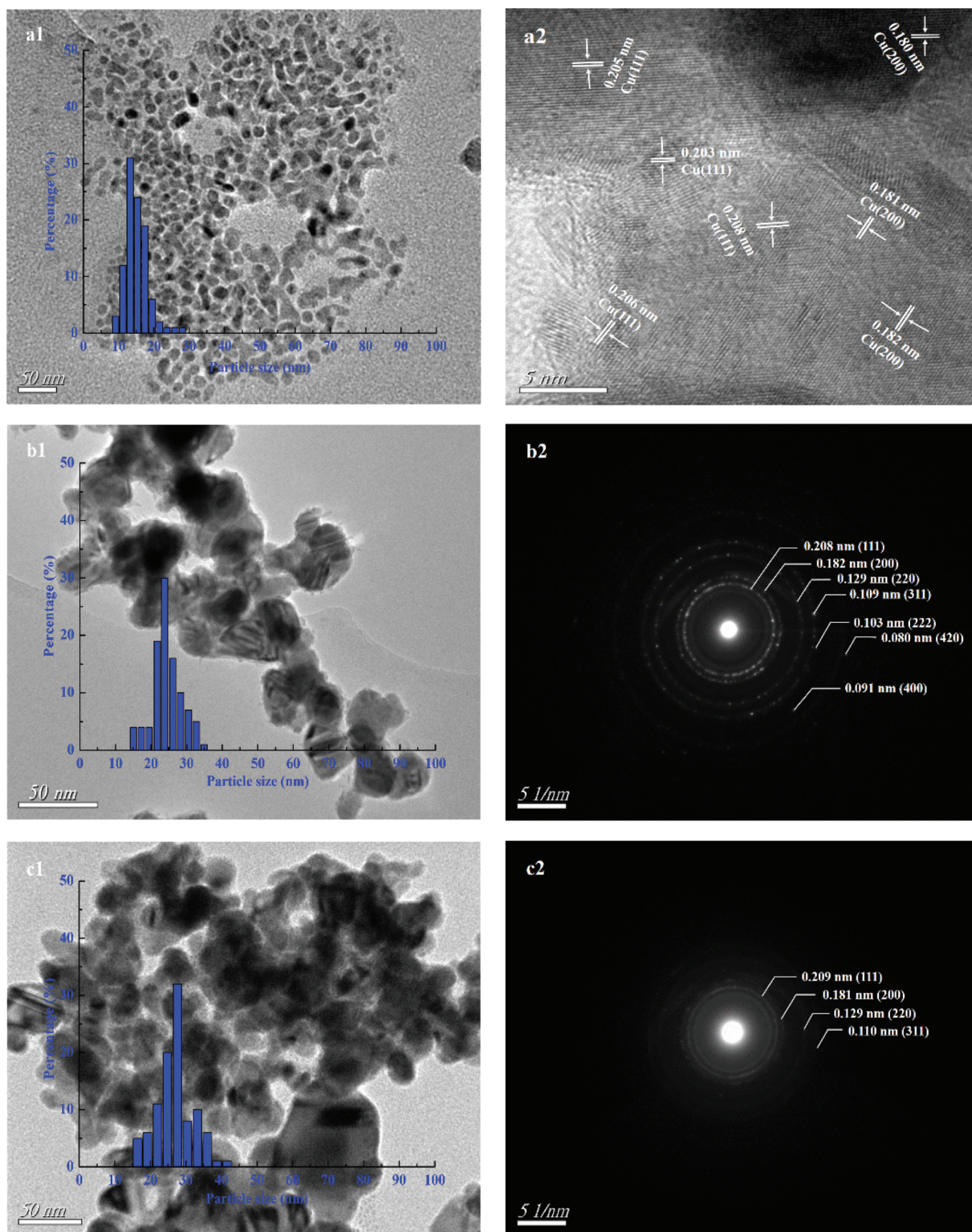


Figure 2. Continued.

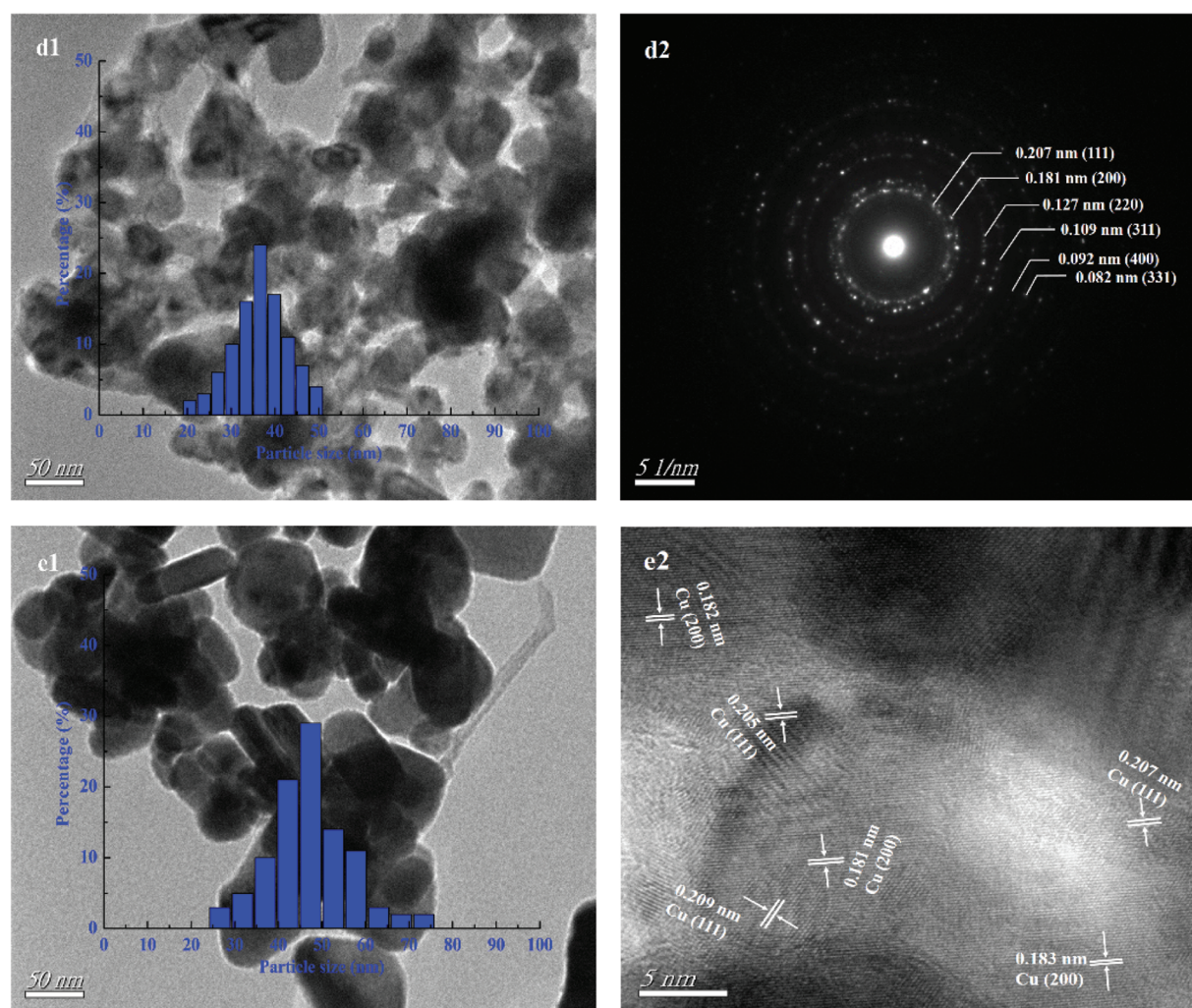


Figure 2. TEM, HRTEM, and SAED images of (a1, a2) Cu_{CA} , (b1, b2) Cu_{CTAB} , (c1, c2) Cu_{Tween} , (d1, d2) Cu_{PEG} , and (e1, e2) Cu_0 samples.

3.3. XPS Analysis

The XPS measurement was employed to determine the surface chemical states of the copper nanoparticles. Figure 3(a) shows the XPS spectra of $\text{Cu}2p$ regions.

The binding energies of $\text{Cu}2p_{1/2}$ and $\text{Cu}2p_{3/2}$ are summarized in Table I.

For the Cu_{CA} , Cu_{CTAB} , Cu_{Tween} , Cu_{PEG} , and Cu_0 nanoparticles, the binding energies values of $\text{Cu}2p_{1/2}$ and $\text{Cu}2p_{3/2}$

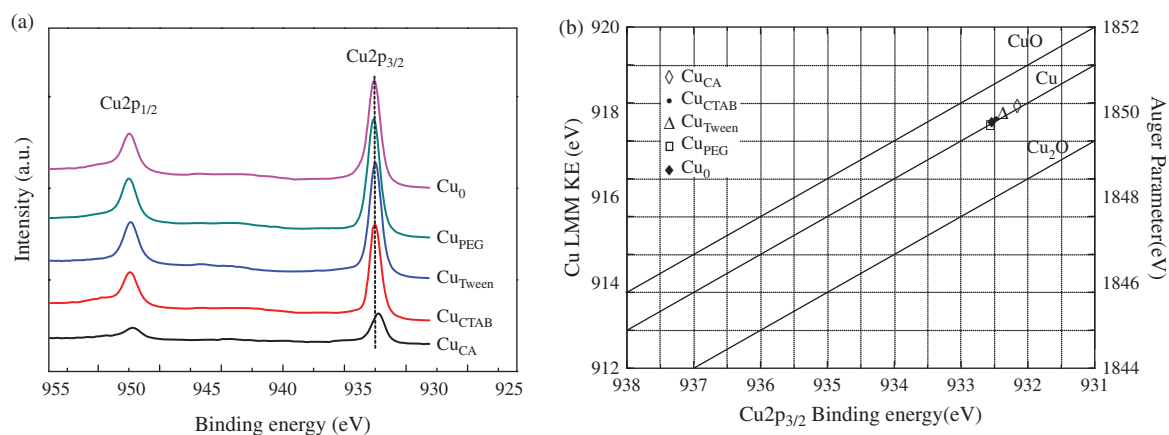


Figure 3. (a) XPS spectra of Cu_{CA} , Cu_{CTAB} , Cu_{Tween} , Cu_{PEG} , and Cu_0 samples and (b) Wagner plots of copper species.

were 952.2, 932.2; 952.4, 932.5; 952.3, 932.4; 952.5, 932.6; and 952.5, 932.6 eV, respectively. For the Cu_{CA} , Cu_{CTAB} , and Cu_{Tween} nanoparticle catalyst, the $\text{Cu}2p_{3/2}$ peaks slightly shifted to low binding energies as compared with those of standard Cu^0 (932.6 eV) and Cu^+ (932.4 eV), referenced to $\text{C}1s$ at 284.6 eV.³⁹ There was no a satellite peak of Cu^{2+} at *ca.* 942 eV found in the $\text{Cu}2p_{1/2}$ and $\text{Cu}2p_{3/2}$ spectra of the copper nanoparticles, revealing that the Cu^{2+} species were completely reduced to low valence states, metallic Cu^0 or Cu^+ , while using hydrazine hydrate as the reductant.

The metallic Cu^0 and Cu^+ species cannot be distinguished directly in accordance with their binding energy values because the standard binding energy values of metallic Cu^0 and Cu^+ are almost similar. To ascertain the surface chemical states of the copper nanoparticles, the Wagner plots are drawn and shown in Figure 3(b) by taking the kinetic energy (KE) of the Auger transition and the $\text{Cu}2p_{3/2}$ binding energy as *Y* and *X* axes, respectively. The data for Cu , Cu_2O , and CuO reference samples were taken from Refs. [40, 41]. The Auger parameters of the samples fell on the line of metallic copper, indicating that the copper species present on the surfaces of copper

nanoparticles were metallic Cu^0 . The as-prepared metallic copper nanoparticles were stable under our present treatment procedures.

3.4. Oxidation of 1,2-Propanediol Catalyzed by Copper Nanoparticles

3.4.1. Effect of Particle Sizes of Copper Nanoparticles

The catalytic oxidation of 1,2-propanediol over metallic copper nanoparticles with different particle sizes was carried out in a NaOH aqueous solution at 200 °C and 1 MPa O_2 for 4 h. The results are listed in Table I. When the copper nanoparticles were used as the catalysts, 1,2-propanediol was effectively oxidized with the conversions of more than 77.1%. The main products were lactic, acetic, and formic acids.

According to the carbon balance, in addition to the three detected products, a small amount of carbonate was probably formed in the presence of sodium hydroxide. In our previous work, the carbon mole ratios of the resultant acetic acid to formic acid were close to 2:1 in all the experiments.^{35,37,42} However, the selectivity ratios of acetic acid to formic acid were higher than 2:1 in our present research, suggesting that a part of formic acid was

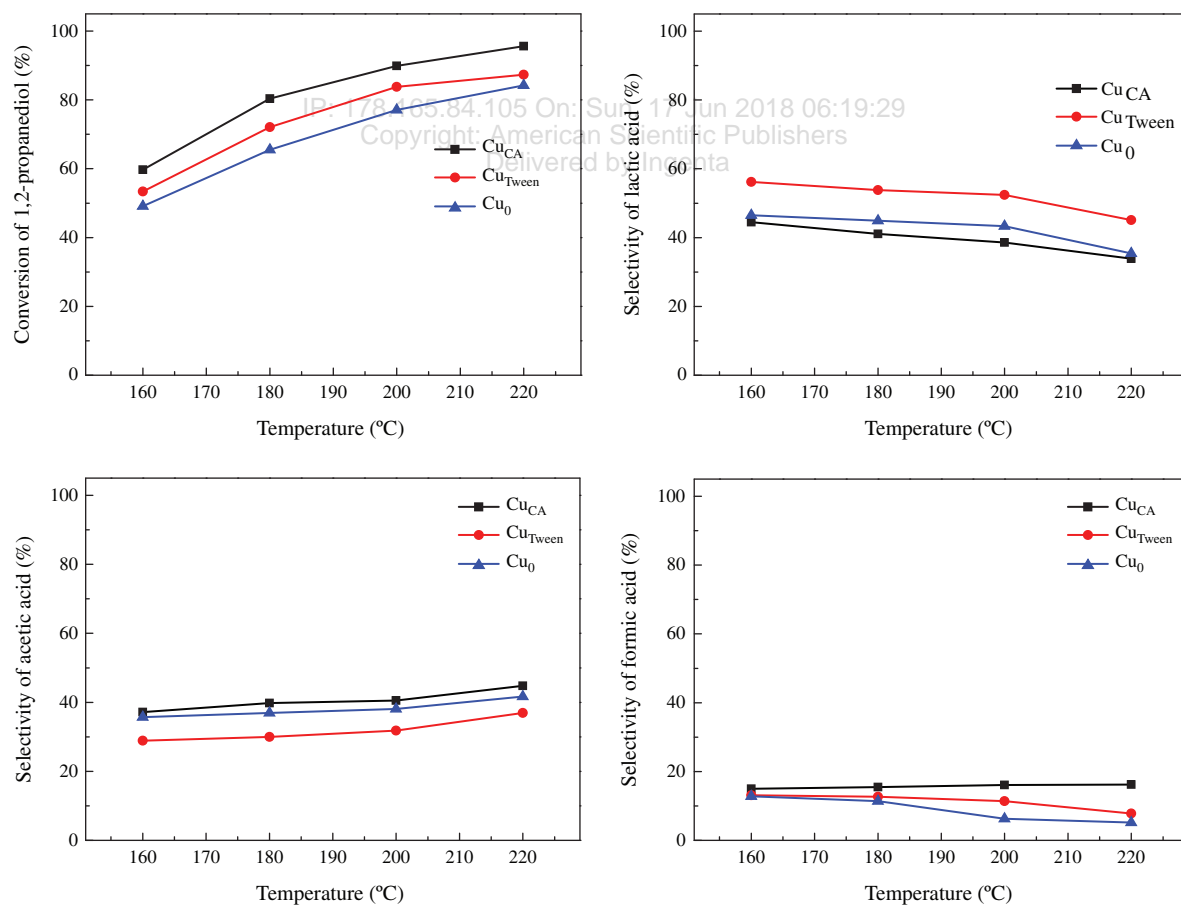


Figure 4. Effect of reaction temperature on the catalytic oxidation of 1,2-propanediol over Cu_{CA} , Cu_{Tween} and Cu_0 nanoparticles. Reaction conditions: 1,2-propanediol aqueous solution, 200 mL, 0.14 mol L⁻¹; NaOH concentration, 0.28 mol L⁻¹; O_2 pressure, 1.0 MPa; catalyst loading, 0.1 g; reaction time, 4 h; and stirring rate, 600 rpm.

probably oxidized with O_2 to CO_2 under the present reaction conditions.

According to the 1,2-propanediol conversions and TOF values, it was found that the oxidation rates of 1,2-propanediol over the copper nanoparticles were in an order of $Cu_{CA} > Cu_{CTAB} > Cu_{Tween} > Cu_{PEG} > Cu_0$. Small-sized copper nanoparticles had higher catalytic activity for the oxidation of 1,2-propanediol than large-sized ones. The maximum lactic acid selectivity of 52.4% was obtained over the Cu_{Tween} nanoparticle catalyst. It is concluded that the copper nanoparticles with the sizes centered at 26.9 nm favored the oxidation of 1,2-propanediol to lactic acid. The copper nanoparticles with small particle sizes enhanced the oxidation of 1,2-propanediol to acetic and formic acids because high total selectivity of acetic and formic acids was obtained over the small-sized copper nanoparticles. Considering that a lower selectivity ratio of formic acid to acetic acid was obtained over the large-sized copper nanoparticles, it could be concluded that the copper nanoparticles with large particle sizes caused the oxidation of resultant formic acid to CO_2 . The particle size effect was obvious for the oxidation of 1,2-propanediol to the corresponding carboxylic acids.

In the following sections, we selected Cu_{CA} , Cu_{Tween} , and Cu_0 as the model catalysts to investigate the effect of other reaction parameters on the oxidation of 1,2-propanediol.

3.4.2. Effect of Reaction Temperature

Figure 4 shows the conversions of 1,2-propanediol and the selectivities of lactic, acetic, and formic acids in the oxidation of 1,2-propanediol catalyzed by Cu_{CA} , Cu_{Tween} , and Cu_0 nanoparticles at different reaction temperatures. After reacting for 4 h at 1.0 MPa of O_2 over the Cu_{CA} , Cu_{Tween} , and Cu_0 catalysts, upon increasing the reaction temperatures from 160 to 220 °C, the conversions of 1,2-propanediol increased to 95.6%, 87.3%, and 84.2%, respectively, and the selectivities of lactic acid decreased from 44.5% to 33.9%, 56.2% to 45.1%, and 46.5% to 35.4%, respectively. The selectivities of acetic acid increased from 37.2% to 44.8%, 28.9% to 36.9%, 35.7% to 41.7%. The selectivities of formic acid over the Cu_{CA} catalyst were around 16%. However, over the Cu_{Tween} and Cu_0 catalysts, the selectivities of formic acid decreased from 13.1% to 7.8% and from 12.8% to 5.2%, respectively. The results indicated that a low reaction temperature favored

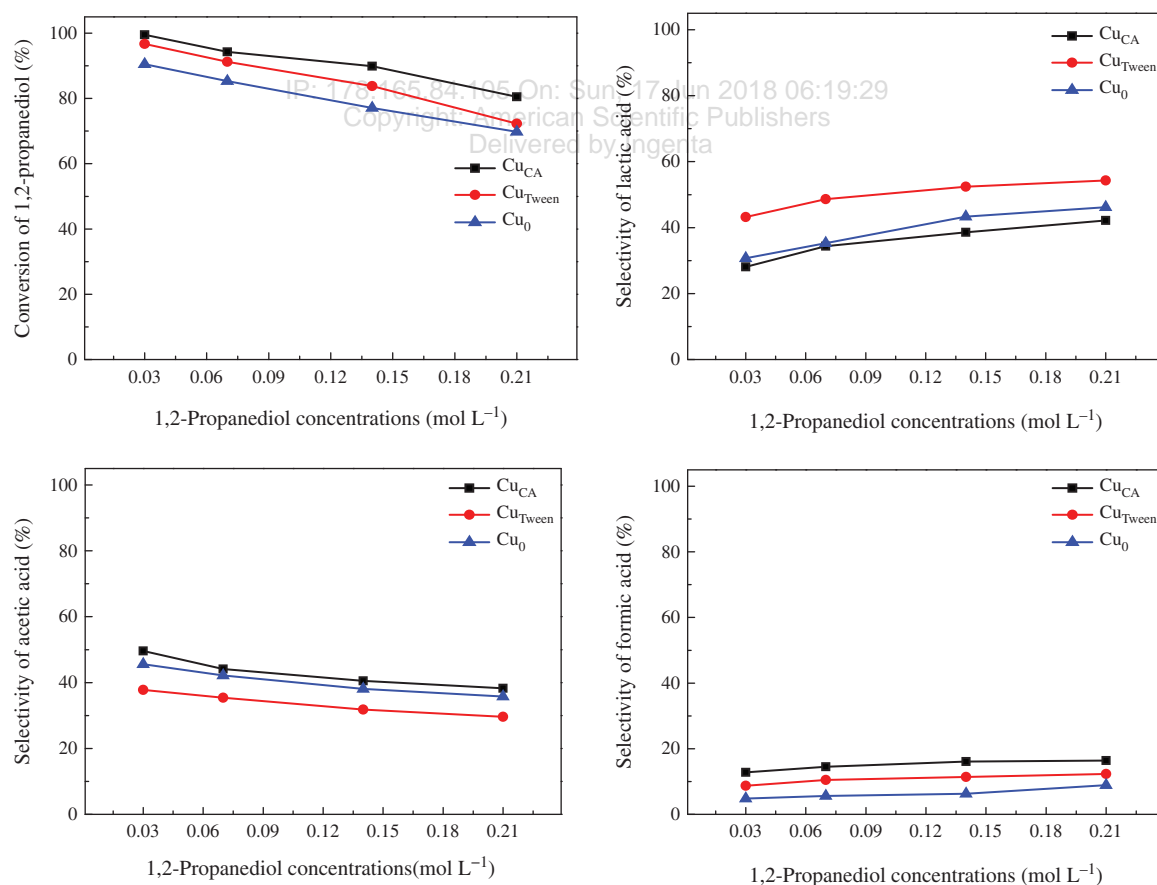


Figure 5. Effect of 1,2-propanediol concentration on the catalytic oxidation of 1,2-propanediol over Cu_{CA} , Cu_{Tween} and Cu_0 nanoparticles. Reaction conditions: 1,2-propanediol aqueous solution, 200 mL; NaOH concentration, 0.28 mol L⁻¹; O_2 pressure, 1.0 MPa; catalyst loading, 0.1 g; reaction temperature, 200 °C; reaction time, 4 h; and stirring rate, 600 rpm.

the oxidation of 1,2-propanediol to lactic acid while a high reaction temperature was beneficial to the formation of acetic acid. Furthermore, it was also found that the total selectivities of lactic, acetic, and formic acids decreased to 94.9%, 89.8%, and 82.3%, respectively, upon increasing the reaction temperature to 220 °C. It is suggested that the degradation degree of formic acid increased upon increasing the reaction temperature.

3.4.3. Effect of 1,2-Propanediol Concentration

After reacting at 200 °C and 1.0 MPa of O₂ for 4 h over the Cu_{CA}, Cu_{Tween}, and Cu₀ catalysts, upon increasing the 1,2-propanediol concentrations from 0.03 to 0.21 mol L⁻¹, the conversions of 1,2-propanediol decreased from 99.5% to 80.5%, 96.7% to 72.3%, and 90.5% to 69.8%, respectively (Fig. 5). The selectivities of lactic acid increased to 42.2%, 54.3%, and 46.2%, respectively. The selectivities of acetic acid decreased from 49.6% to 38.3%, 37.8% to 29.6%, and 45.6% to 35.8% while the selectivities of formic acid slightly increased to 16.4%, 12.3%, and 8.9%, respectively. However, the total selectivities of lactic, acetic, and formic acids increased upon increasing 1,2-propanediol concentrations. It could be explained as that at a low 1,2-propanediol concentration, more catalytic active

sites were available on the surfaces of the copper nanoparticles, increasing the degradation degree of formic and acetic acids.

3.4.4. Effect of O₂ Pressure

When the reaction was carried out at 200 °C for 4 h over the Cu_{CA}, Cu_{Tween}, and Cu₀ nanoparticle catalysts, upon increasing the O₂ pressures to 1.5 MPa, the 1,2-propanediol conversions increased to 96.5%, 94.2%, and 86.2%, respectively (Fig. 6). The maximum selectivities of lactic acid of 38.6%, 52.4%, and 43.3% were obtained at the O₂ pressure of 1.0 MPa. The selectivities of acetic and formic acids were around 44%, 38%, 43%; 17%, 13%, 10%, respectively. The total selectivities of lactic, acetic, and formic acids decreased upon increasing the O₂ pressure. The results indicated that a high O₂ pressure was beneficial for the conversion of 1,2-propanediol due to more activated oxygen available. Excessive O₂ also caused the mineralization of the resultant acids.

3.4.5. Effect of NaOH Concentration

When the oxidation of 1,2-propanediol was catalyzed by Cu_{CA} and Cu_{Tween} nanoparticle catalysts at 1.0 MPa of

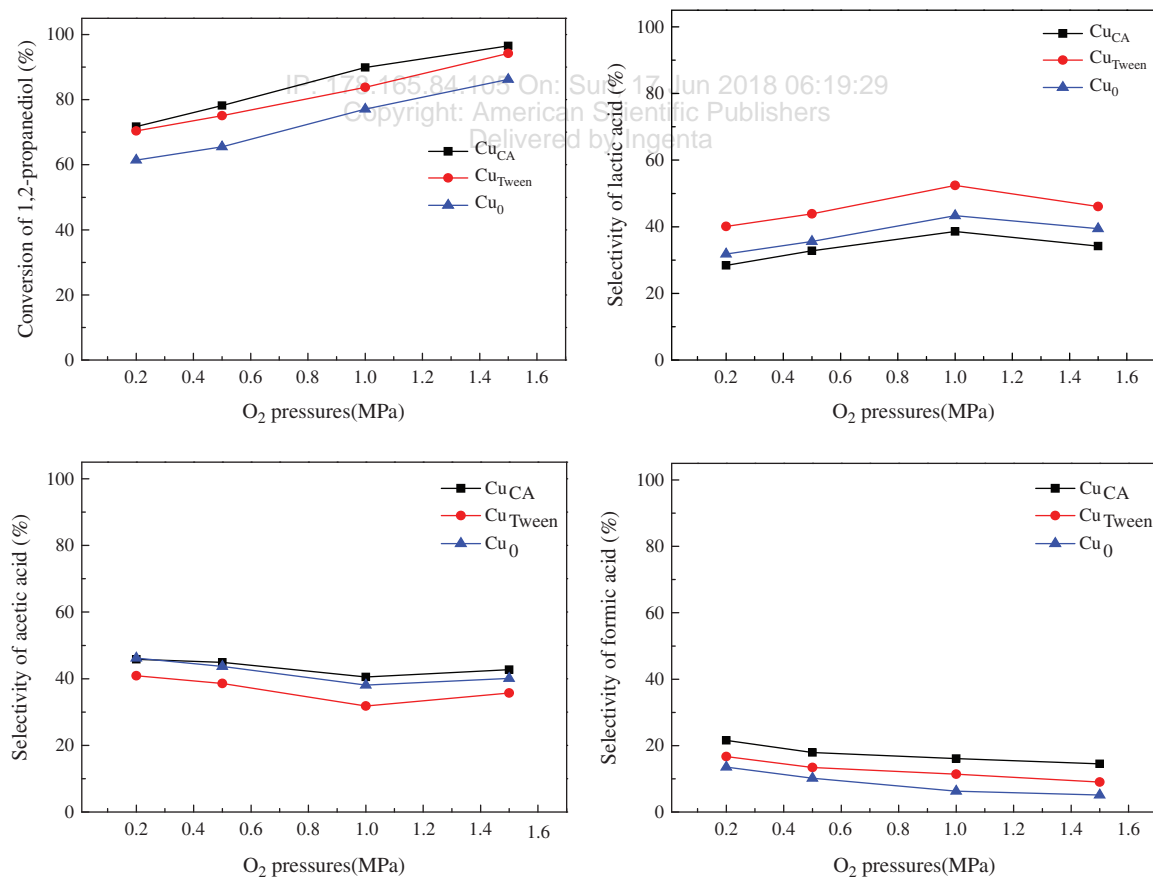


Figure 6. Effect of O₂ pressure on the catalytic oxidation of 1,2-propanediol over Cu_{CA}, Cu_{Tween} and Cu₀ nanoparticles. Reaction conditions: 1,2-propanediol aqueous solution, 200 mL, 0.14 mol L⁻¹; NaOH concentration, 0.28 mol L⁻¹; catalyst loading, 0.1 g; reaction temperature, 200 °C; reaction time, 4 h; and stirring rate, 600 rpm.

Table II. Effect of NaOH concentration on the catalytic oxidation of 1,2-propanediol over Cu_{CA} and Cu_{Tween} catalysts^a.

Catalysts	NaOH concentrations (mol L ⁻¹)	Conversions (%)	Selectivities (%)		
			Lactic acid	Acetic acid	Formic acid
Cu _{CA}	0.14	73.2	32.4	45.4	17.7
	0.28	89.9	38.6	40.5	16.1
	0.42	92.4	43.1	38.3	14.8
	0.56	92.6	43.1	38.0	14.4
Cu _{Tween}	0.14	68.2	41.5	39.3	13.5
	0.28	83.8	52.4	31.8	11.4
	0.42	89.7	53.7	29.9	10.9
	0.56	90.3	53.9	29.4	10.2

Notes: ^aReaction conditions: 1,2-propanediol aqueous solution, 200 mL, 0.14 mol L⁻¹; O₂ pressure, 1.0 MPa; catalyst loading, 0.1 g; reaction temperature, 200 °C; reaction time, 4 h; and stirring rate, 600 rpm.

O₂ and 200 °C for 4 h, upon increasing the NaOH concentration to 0.56 mol L⁻¹, the conversions of 1,2-propanediol increased to 92.6% and 90.3% and the selectivities of lactic acid increased to 43.1% and 53.9%, respectively (Table II). The selectivities of acetic and formic acids decreased to 38.0%, 14.4%; 29.4%, 10.2%, respectively. The results revealed that a high NaOH concentration favored the conversion of 1,2-propanediol to lactic acid while a low NaOH concentration was beneficial to the formation of acetic and formic acids. It was also found that when the NaOH concentration was increased to 0.56 mol L⁻¹, the conversion of 1,2-propanediol and selectivities of products were close to those with the NaOH concentration of 0.42 mol L⁻¹. To obtain high product yields, the mole ratio of NaOH to 1,2-propanediol of 3:1 was appropriate.

3.4.6. Effect of Catalyst Loading

The conversions of 1,2-propanediol and the selectivities of lactic acid, acetic acid, and formic acid in the catalytic oxidation of 1,2-propanediol over Cu_{CA} and Cu_{Tween} nanoparticle catalysts with different catalyst loadings are

Table III. Effect of catalyst loading on the catalytic oxidation of 1,2-propanediol over Cu_{CA} and Cu_{Tween} catalysts^a.

Catalysts	Catalyst loadings (g)	Conversions (%)	Selectivities (%)		
			Lactic acid	Acetic acid	Formic acid
Cu _{CA}	0.05	78.4	35.2	43.7	16.8
	0.10	89.9	38.6	40.5	16.1
	0.15	92.2	36.4	42.9	15.6
	0.20	92.8	34.5	43.2	15.3
Cu _{Tween}	0.05	75.1	43.7	38.2	13.6
	0.10	83.8	52.4	31.8	11.4
	0.15	85.6	50.6	32.9	10.8
	0.20	87.4	49.2	33.5	10.1

Notes: ^aReaction conditions: 1,2-propanediol aqueous solution, 200 mL, 0.14 mol L⁻¹; NaOH concentration, 0.28 mol L⁻¹; O₂ pressure, 1.0 MPa; reaction temperature, 200 °C; reaction time, 4 h; and stirring rate, 600 rpm.

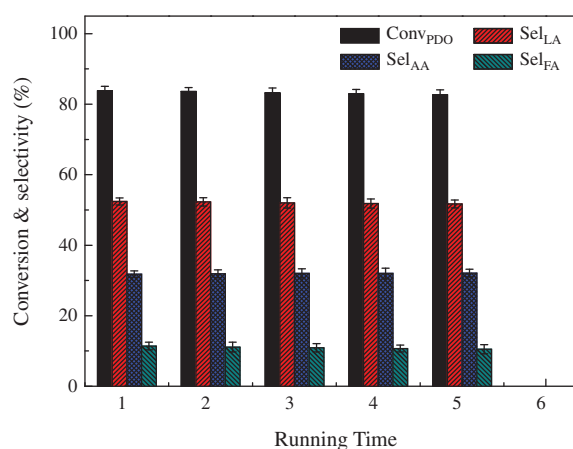
listed in Table III. After reacting at 200 °C for 4 h, upon increasing catalyst loadings from 0.05 to 0.2 g, the 1,2-propanediol conversions over Cu_{CA} and Cu_{Tween} catalysts increased to 92.8% and 87.4%, respectively. The selectivities of lactic, acetic, and formic acids were around 36%, 42%, 16%; 50%, 33%, 11%, respectively. High catalyst loading favored the conversion of 1,2-propanediol to the acids.

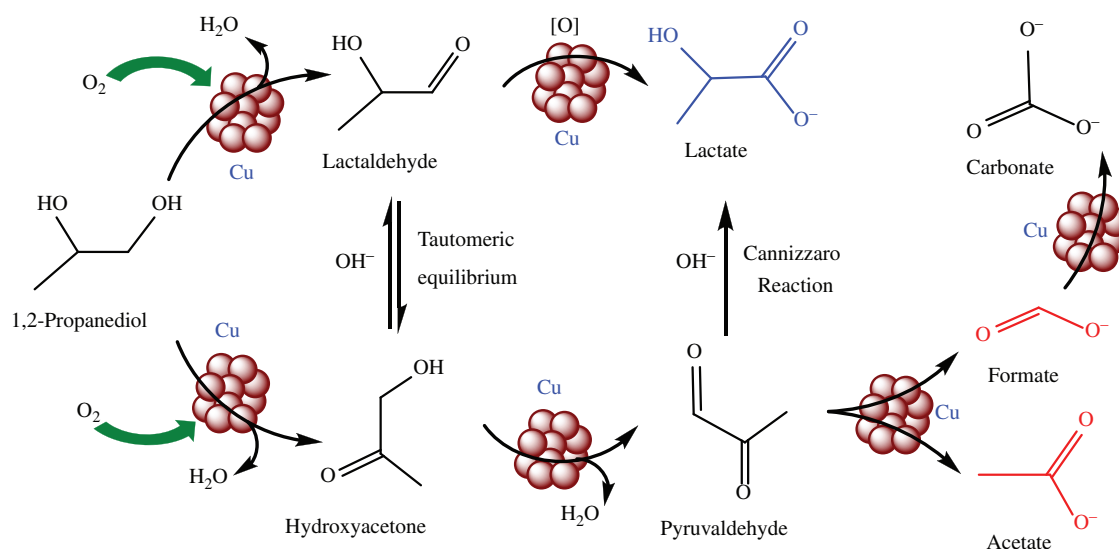
3.5. Catalyst Recycling Performance

The recycling performance of the Cu_{Tween} nanoparticle catalyst for the catalytic oxidation of 1,2-propanediol was also investigated. After reacting at 200 °C for 4 h, the used catalyst was centrifugated, washed with anhydrous ethanol, and dried at 40 °C in a vacuum oven overnight before next running. As shown in Figure 7, for the fresh Cu_{Tween} catalyst, the conversion of 1,2-propanediol and the selectivity of lactic acid were 83.8% and 52.4%, respectively. After recycling for five times, there was no obvious change in the 1,2-propanediol conversion and product selectivities, indicating that the Cu_{Tween} catalyst exhibited good recycling performance.

3.6. Reaction Routes

The reaction routes for the oxidation of 1,2-propanediol are complex, two possible reaction routes over copper nanoparticle catalysts in alkaline solution are suggested as Scheme 1.^{30, 37, 43} Through the first route, metallic copper nanoparticles catalyze the oxidation of the primary hydroxyl group of 1,2-propanediol to form lactaldehyde. Then the resultant lactaldehyde can be oxidized to lactate. Through the second route, metallic copper nanoparticles catalyze the oxidation of the secondary hydroxyl group. 1,2-Propanediol is oxidized to hydroxyacetone. And then, the resultant hydroxyacetone is oxidized to pyruvaldehyde,


Figure 7. Recycling performance of the Cu_{Tween} nanoparticle catalyst for the catalytic oxidation of 1,2-propanediol. Reaction conditions: 1,2-propanediol aqueous solution, 200 mL, 0.14 mol L⁻¹; NaOH concentration, 0.28 mol L⁻¹; O₂ pressure, 1.0 MPa; catalyst loading, 0.1 g; reaction temperature, 200 °C; reaction time, 4 h; and stirring rate, 600 rpm.



Scheme 1. Reaction routes for catalytic oxidation of 1,2-propanediol over metallic Cu⁰ nanoparticle catalysts in an alkaline solution.

which can be further oxidized and cleaved to acetate anion and formate anion, accompanied with the formation of carbonate anions.⁴⁴ Meanwhile, hydroxyacetone can be transformed to lactaldehyde via the tautomeric equilibrium. Then, the resultant lactaldehyde is oxidized to lactate. Pyruvaldehyde can also be converted to lactate in an alkaline solution through the Cannizzaro reaction. The intermediates, such as lactaldehyde, hydroxyacetone, and pyruvaldehyde, were not detected under our present experimental conditions, indicating that the intermediates could be rapidly converted to subsequent chemicals.

4. CONCLUSIONS

The copper nanoparticles with the average particle sizes ranging from 15.2 nm to 47.1 nm were successfully prepared by a wet chemical reduction method. The product selectivities in the catalytic oxidation of 1,2-propanediol were significantly affected by the particle size of the metallic Cu⁰ nanoparticle. When the Cu_{CA} nanoparticle was used as the catalyst, after reacting at 1.0 MPa of O₂ and 200 °C for 4 h in an alkaline solution, the selectivities of lactic, acetic, and formic acids were 38.6%, 40.5%, and 16.1%, respectively, at the 1,2-propanediol conversion of 89.9%. Carrying out the reaction over Cu_{Tween} nanoparticle catalyst, the 1,2-propanediol conversion was 83.8% with the lactic, acetic, and formic acid selectivities of 52.4%, 31.8%, and 11.4%, respectively. The copper nanoparticles effectively catalyzed the oxidation of 1,2-propanediol to lactic, acetic, and formic acids and exhibited good recycling performance. The copper nanoparticles with a lower cost have potential application in the oxidation of 1,2-propanediol to high-valued organic acids.

Acknowledgments: The work was financially supported by the funds from National Natural Science

Foundation of China (21506078 and 21506082) and Science and Technology Department of Jiangsu Province of China (BY2014123-10).

References and Notes

1. Y. Muranak, A. Iwai, I. Hasegaw, and K. Mae, *Chem. Eng. J.* 234, 189 (2013).
2. J. Mazumder and H. I. de Lasa, *Chem. Eng. J.* 293, 232 (2016).
3. Y. W. Weldu and G. Assefa, *Environ. Impact Assess Rev.* 60, 75 (2016).
4. P. Parthasarathy and K. S. Narayanan, *Renew. Energ.* 66, 570 (2014).
5. B. Hejazi, J. R. Grace, X. Bi, and A. Mahecha-Botero, *Fuel* 117, 1256 (2014).
6. H. de Lasa, E. Salaices, J. Mazumder, and R. Lucky, *Chem. Rev.* 111, 5404 (2011).
7. G. W. Huber, S. Iborra, and A. Corma, *Chem. Rev.* 106, 4044 (2006).
8. H. W. Tan, A. R. Abdul Aziz, and M. K. Aroua, *Renew. Sust. Energ. Rev.* 27, 118 (2013).
9. Y. H. Feng, H. B. Yin, L. Q. Shen, A. L. Wang, Y. T. Shen, and T. S. Jiang, *Chem. Eng. Technol.* 36, 73 (2013).
10. M. Lee, Y. K. Hwang, J. S. Chang, H. J. Chae, and D. W. Hwang, *Catal. Commun.* 84, 5 (2016).
11. L. Q. Shen, H. B. Yin, A. L. Wang, and Y. H. Feng, *Chem. Eng. J.* 180, 277 (2012).
12. X. Y. Liao, Y. L. Zhu, S. G. Wang, and Y. W. Li, *Fuel Process. Technol.* 90, 988 (2009).
13. S. Gil, M. Marchena, L. Sánchez-Silva, A. Romero, P. Sánchez, and J. L. Valverde, *Chem. Eng. J.* 178, 423 (2011).
14. Y. H. Feng, H. B. Yin, D. Z. Gao, A. L. Wang, L. Q. Shen, and M. J. Meng, *J. Catal.* 316, 67 (2014).
15. Y. H. Feng, H. B. Yin, A. L. Wang, D. Z. Gao, X. Y. Zhu, L. Q. Shen, and M. J. Meng, *Appl. Catal. A: Gen.* 482, 49 (2014).
16. G. Y. Yang, Y. H. Ke, H. F. Ren, C. L. Liu, R. Z. Yang, and W. S. Dong, *Chem. Eng. J.* 283, 759 (2016).
17. P. Maki-Arvela, I. L. Simakova, T. Salmi, and D. Y. Murzin, *Chem. Rev.* 114, 1909 (2014).
18. K. L. Wasewar, A. A. Yawalkar, J. A. Moulijn, and V. G. Pangarkar, *Ind. Eng. Chem. Res.* 43, 5969 (2004).
19. J. Zhang, M. Sun, X. Liu, and Y. Han, *Catal. Today* 233, 77 (2014).

20. T. Yonezawa, K. Kawai, H. Kawakami, and T. Narushima, *Bull. Chem. Soc. Jpn.* 89, 1230 (2016).
21. S. Li, X. Chen, J. Chen, and H. Gong, *Bull. Chem. Soc. Jpn.* 89, 794 (2016).
22. Y. Hang, H. Yin, Y. Ji, Y. Liu, Z. Lu, A. Wang, L. Shen, and H. Yin, *J. Nanosci. Nanotechnol.* 17, 5539 (2017).
23. H. Abe, J. Liu, and K. Ariga, *Mater. Today* 19, 12 (2016).
24. X. Wang, J. Feng, Y. Bai, Q. Zhang, and Y. Yin, *Chem. Rev.* 116, 10983 (2016).
25. H. X. Yin, H. B. Yin, A. Wang, L. Shen, Y. Liu, and Y. Zheng, *J. Nanosci. Nanotechnol.* 17, 1255 (2017).
26. L. Shen, H. X. Yin, H. B. Yin, S. Liu, and A. Wang, *J. Nanosci. Nanotechnol.* 17, 780 (2017).
27. Y. Ji, J. Gao, H. Yin, A. Wang, T. Jiang, G. Wu, and Z. Wu, *J. Nanosci. Nanotechnol.* 15, 3967 (2015).
28. W. Xue, Y. Feng, H. Yin, S. Liu, A. Wang, and L. Shen, *J. Nanosci. Nanotechnol.* 16, 9621 (2016).
29. L. Prati and M. Rossi, *J. Catal.* 176, 552 (1998).
30. N. Dimitratos, J. A. Lopez-Sanchez, S. Meenakshisundaram, J. M. Anthonykutti, G. Brett, A. F. Carley, S. H. Taylor, D. W. Knight, and G. J. Hutchings, *Green Chem.* 11, 1209 (2009).
31. Y. Ryabenkova, Q. He, P. J. Miedziak, N. F. Dummer, S. H. Taylor, A. F. Carley, D. J. Morgan, N. Dimitratos, D. J. Willock, D. Bethell, D. W. Knight, D. Chadwick, C. J. Kiely, and G. J. Hutchings, *Catal. Today* 203, 139 (2013).
32. Y. Ryabenkova, P. J. Miedziak, N. F. Dummer, S. H. Taylor, N. Dimitratos, D. J. Willock, D. Bethell, D. W. Knight, and G. J. Hutchings, *Top. Catal.* 55, 1283 (2012).
33. M. B. Griffin, A. A. Rodriguez, M. M. Montemore, J. R. Monnier, C. T. Williams, and J. W. Medlin, *J. Catal.* 307, 111 (2013).
34. E. Redina, A. Greish, R. Novikov, A. Strelkova, O. Kirichenko, O. Tkachenko, G. Kapustin, I. Sinev, and L. Kustov, *Appl. Catal. A: Gen.* 491, 170 (2015).
35. Y. H. Feng, W. P. Xue, H. B. Yin, M. J. Meng, A. L. Wang, and S. X. Liu, *RSC Adv.* 5, 106918 (2015).
36. D. Tongsakul, S. Nishimura, and K. Ebitani, *J. Phys. Chem. C* 118, 11723 (2014).
37. Y. H. Feng, H. B. Yin, A. L. Wang, and W. P. Xue, *J. Catal.* 326, 26 (2015).
38. M. B. Gawande, A. Goswami, F. X. Felpin, T. Asefa, X. Huang, R. Silva, X. Zou, R. Zboril, and R. S. Varma, *Chem. Rev.* 116, 3722 (2016).
39. S. Poulston, P. M. Parlett, P. Stone, and M. Bowker, *Surf. Interface Anal.* 24, 811 (1996).
40. D. Z. Zhang, H. B. Yin, J. J. Xue, C. Ge, T. S. Jiang, L. B. Yu, and Y. T. Shen, *Ind. Eng. Chem. Res.* 48, 11220 (2009).
41. W. L. Dai, Q. Sun, J. F. Deng, D. Wu, and Y. H. Sun, *Appl. Surf. Sci.* 177, 172 (2001).
42. W. P. Xue, H. B. Yin, Z. P. Lu, Y. H. Feng, A. L. Wang, S. X. Liu, L. Q. Shen, and X. Y. Jia, *Catal. Lett.* 146, 1139 (2016).
43. H. Ma, X. Nie, J. Cai, C. Chen, J. Gao, H. Miao, and J. Xu, *Sic. China Chem.* 53, 1497 (2010).
44. C. A. Ramírez-López, J. R. Ochoa-Gómez, M. Fernández-Santos, O. Gómez-Jiménez-Aberasturi, A. Alonso-Vicario, and J. Torrecilla-Soria, *Ind. Eng. Chem. Res.* 49, 6270 (2010).

Received: 16 March 2017. Accepted: 29 April 2017.

IP: 178.165.84.105 On: Sun, 17 Jun 2018 06:19:29
Copyright: American Scientific Publishers
Delivered by Ingenta